Knudsen Diffusivities and Properties of Structures of Unidirectional Fibers

Manolis M. Tomadakis and Stratis V. Sotirchos
Dept. of Chemical Engineering, University of Rochester, Rochester, NY 14627

Effective Knudsen diffusion coefficients are presented for fibrous structures consisting of parallel, nonoverlapping or partially overlapping fibers. They are computed by means of a Monte Carlo simulation scheme which is employed to determine the mean square displacement of molecules travelling in the interior of the porous medium for large travel times. The results show that structures of parallel, nonoverlapping fibers have smaller effective diffusion coefficients parallel to the fibers than structures of parallel, randomly overlapping fibers of the same porosity and fiber radius, but larger in directions perpendicular to the fibers. Partially overlapping fiber structures are found to exhibit behavior intermediate to those of the two extreme cases. Molecular trajectory computations are also used to obtain results for the structural properties of partially overlapping fiber structures (e.g., porosity and internal surface area, accessible porosity and internal surface area, and percolation threshold), which are compared with some results of the literature for the equivalent problem of partially overlapping disks on a plane.

Introduction

In a previous study (Tomadakis and Sotirchos, 1991), we investigated the problem of Knudsen diffusion in porous media whose structure can be represented by populations of randomly overlapping fibers of various orientation distributions. The axes of the fibers were randomly distributed in two or three directions, i.e., parallel to a plane or in the three-dimensional space without preferred orientation (d-directional ($d=2$ or 3), random fiber structures), or grouped into d ($d=1$, 2, or 3) mutually perpendicular bundles of parallel, randomly overlapping fibers (d-directional, parallel fiber structures). Effective Knudsen diffusivities were estimated by introducing test molecules at random positions in a finite sample (unit cell) of the porous medium and computing their mean square displacement for large travel times, as they travelled independently in the pore space. Using a method proposed by Burganos and Sotirchos (1989c), the computed molecular trajectories were also used to determine the porosity, internal surface area, and accessibility characteristics of the fiber structures.

The results of our previous study led to some very interesting conclusions about the effects of the orientational distribution of the fibers on the effective diffusivity and the accessibility of the fibrous beds. It was found, for example, that the effective Knudsen diffusivity depended strongly on the distribution of the orientation of the fibers at low and intermediate porosity values, but it was independent of the orientation of the fibers in two or three directions, that is, on whether they were randomly distributed or grouped into two or three bundles of parallel fibers. The percolation threshold, i.e., the porosity below which the void space forms only finite regions and mass transport cannot take place, decreased with increasing directionality—while the effective diffusivity increased—from about 0.33 for unidirectional fibers (for diffusion perpendicularly to the fibers) to 0.11 for bidirectional structures and 0.04 for tridirectional structures. This result is of considerable importance for practical applications since it suggests that it may be advantageous to use three-dimensional random or woven structures instead of cloth layups or unidirectional fibers as preforms in practical applications, such as the fabrication of ceramic matrix composites by chemical vapor infiltration.

The fibrous beds that are used in the fabrication of fiber-reinforced ceramic matrix composites and in other applications usually consist of initially nonoverlapping fibers. In the case of densification by deposition of solid material (e.g., by chemical vapor infiltration), the initially nonoverlapping fibers grow into each other as densification proceeds, and a structure of partially overlapping fibers results. The initial porosities of the

Correspondence concerning this article should be addressed to S. V. Sotirchos.

fibrous structures that are used for reinforcement of ceramic composites produced by chemical vapor infiltration vary in the relatively broad range [0.4, 0.85] (Caputo et al., 1985; Naslain et al., 1989). At high porosities, the solid phase that belongs to more than one fibers (that is, the overlapping volume) in a structure of randomly overlapping fibers in a small fraction of the total solid phase. (For example, if the fibers of a randomly overlapping structure with 80% porosity did not overlap, the porosity would be 77.7%.) One could, therefore, argue that our old results for randomly overlapping fibers, such as the variation of the effective diffusivity with the extent of densification, will still be applicable to structures resulting from densification of fibrous beds of high initial porosity.

The fiber overlapping volume in a structure of randomly positioned fibers becomes a significant fraction of the total solid volume at intermediate and low porosity values. It is thus necessary to address the effects of the initial nonoverlapping positioning of the fibers on the evolution of the structural and transport properties of beds of low or intermediate initial porosity. Among the simplest structures of initially nonoverlapping fibers that one can consider is that of unidirectional (parallel) nonoverlapping fibers, positioned in space through some randomizing process. Such a structure is representative, in almost every important detail, of preforms of unidirectional fibers used for reinforcement of ceramic materials (Meyers and Chawla, 1984; Hopkins and Chin, 1986). Densification of these porous media through a solid deposition process gives rise to a partially overlapping fiber structure that can be viewed as consisting of randomly positioned parallel cylinders having a cylindrical hard core of radius equal to that of the fibers of the initial structure.

Past studies on structures of unidirectional, partially overlapping fibers have mainly concentrated on locating their percolation threshold, that is, the porosity or fiber growth level (ratio of fiber radius to hard core radius) below which flow cannot take place in the interior of these porous media perpendicularly to the fibers (Pike and Seager, 1974; Bug et al., 1985; Odagaki and Lax, 1987; Lee and Torquato, 1988b). A few studies have also looked at the variation of the porosity and internal surface area of these structures with the hard core porosity and fiber to hard core radius ratio (Rikvold and Stell, 1985a,b; Lee and Torquato, 1988a; Smith and Torquato, 1988). In most cases, the problem has been studied in the context of the equivalent two-dimensional problem of partially penetrable (overlapping) disks on a plane. However, there has been no work done in the literature on the variation of the effective diffusivity and of the accessibility characteristics of the pore structure of these media with their structural parameters, despite the fact that these quantities play a much more important role in mass transport applications.

A detailed investigation of the dependence of the Knudsen effective diffusivity, structural properties (porosity and surface area), and accessibility characteristics of structures of unidirectional fibers of uniform size on the extent of overlapping and hard core porosity is presented in this research paper. Computation of these quantities is accomplished using the simulation methods employed in our previous study. Since past studies of the percolation behavior of partially overlapping disks or fibers have covered only part of the hard core porosity range, and the percolation threshold is among the most important parameters of an evolving porous structure in a mass transport process, we also present a detailed picture of the percolation behavior of unidirectional fiber structures, obtained using both the molecular trajectory computations and a cluster identification scheme.

Construction of Fibrous Structures and Computation of Effective Knudsen Diffusivities

A scheme based on the Metropolis Monte Carlo method (Metropolis et al., 1953) is used for the construction of finite samples of porous structures consisting of unidirectional, nonoverlapping fibers of uniform size. The fibers are initially positioned in the cubic unit cell in such a way that the traces of the axes of the fibers on the two faces of the cell that are perpendicular to their direction are located at the sites of a regular triangular lattice. Random structures of nonoverlapping fibers are obtained through random sequential moves of the fibers from their initial positions. The trace of the axis of a fiber is randomly displaced to a new position within a square of side h, centered at the previous position of the fiber with its sides parallel to the sides of the unit cell. The new position of the fiber is accepted if the fiber does not overlap with any of the other fibers of the structure. Otherwise, the fiber is left at its previous position, and the process continues with the next fiber. About 500 cycles of fiber moves (during a cycle all fibers are moved or an attempt is made to move them from their previous positions) had to be carried out for the results reported in this study before the resulting random structure could be considered to have reached an equilibrium configuration, away from the initial regular arrangement of the fibers. The side of the square defining the maximum displacement of each fiber, h, was taken equal to the shortest distance between adjacent fibers at the regular triangular spacing.

Periodic boundary conditions are applied in the construction of the unit cell, that is, the distribution of fibers in the unit cell is repeated in all other cells. In this way, a structure spanning the whole space in directions perpendicular to the fibers is generated. The assumption of a periodic unit cell greatly facilitates the construction of the random fiber structure using the Metropolis Monte Carlo scheme since fibers displaced into neighboring cells during the sequential moves process are simply reintroduced into the reference unit cell at the same relative position. A periodic, unidirectional structure of uniformly-sized, nonoverlapping fibers constructed by means by the above procedure is shown in Figure 1A. A structure of randomly (freely) overlapping fibers of the same porosity is shown in Figure 1B. Each figure presents a section of a unit cell with a plane perpendicular to the fibers for 45% porosity and unit cell side to fiber radius ratio equal to 18. For fibers of 1 μm in radius, Figure 1A or Figure 1B would depict an 18 μm $\times$ 18 μm micrograph of the fiber structure.

Nonoverlapping fiber structures cannot exist below the porosity that corresponds to a regular triangular array of closely packed fibers, which, as it is well known, is given by $\epsilon_{ocp} = 1 - \sqrt{3}\pi/6 = 0.093100\cdots$. Another close packing model of unidirectional fibers or disks in two dimensions is that of random close packing, which can be thought of as the densest structure that can be obtained by shaking a container full of parallel, cylindrical rods. By defining the random close packing as the minimum porosity packing that contains no statistically

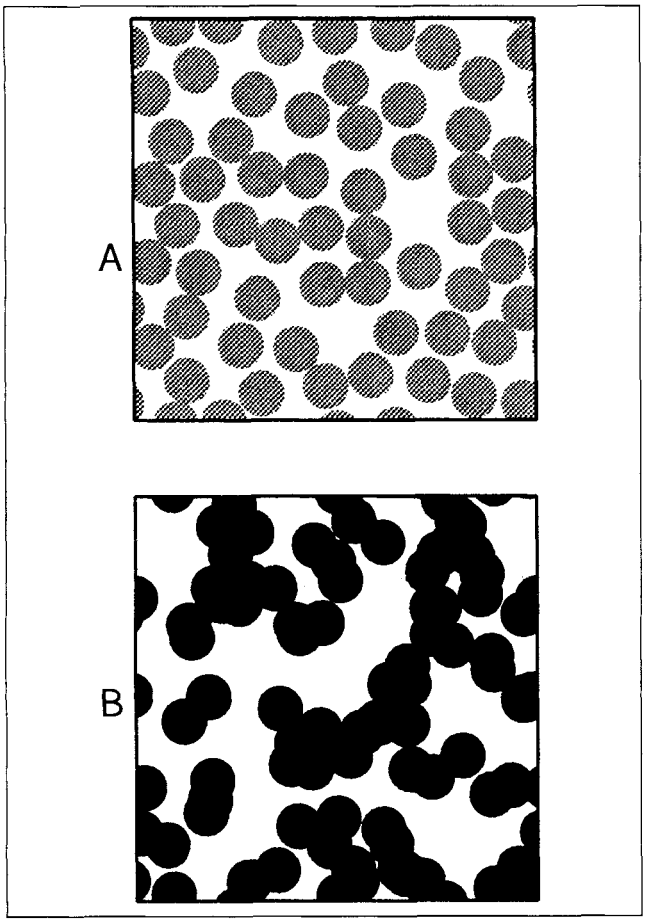

Figure 1. Cross sections of unit cells of structures of (A) nonoverlapping and (B) freely overlapping fibers, each having 45% porosity.

significant short- or long-range order, Berryman (1983) arrived at an estimate of the random close packing porosity, ϵ_{rcp}, of 0.18 ± 0.02. The state of random close packing does not appear to be stable in two dimensions, in contrast to that for spheres in three dimensions, and the experimental estimates of ϵ_{rcp} fall in the rather wide range 0.11–0.18. Our computations will cover the whole range of feasible hard-core porosities (i.e., $[\epsilon_{ocp}, 1]$), but it must be kept in mind that for applications, hard core porosities below ϵ_{rcp} may not be attainable for randomly packed fiber structures.

Partially overlapping fiber structures are obtained from nonoverlapping fiber structures, such as that shown in Figure 1A, by increasing the fiber size by a certain amount. A partially overlapping fiber structure resulting from the structure of Figure 1A after the fibers have been allowed to grow by 25% is shown in Figure 2. For a structure undergoing densification, by chemical vapor infiltration for example, the rings added around the fibers of the original nonoverlapping fiber structure, displayed using solid black pattern, correspond to the material deposited within the preform during the process. It is interesting to point out that the structure of Figure 2 is qualitatively similar to micrographs of partially densified structures reported in the literature (e.g., Hopkins and Chin, 1986). While nonoverlapping or freely overlapping fiber structures can uniquely be identified by their porosity and fiber radius,

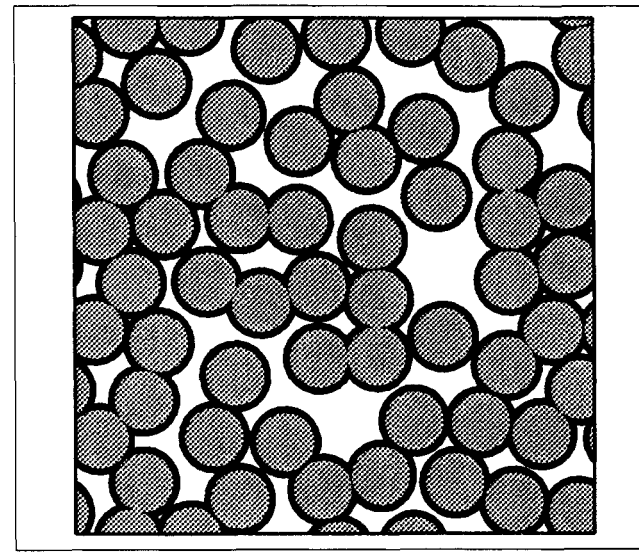

Figure 2. Cross section of a unit cell of the partially-overlapping fiber structure obtained from the structure of Figure 1A when the fiber radius is increased by 25%.

$\epsilon = 0.21$

structures of partially overlapping fibers need for their unique identification the porosity of the nonoverlapping fiber structure from which they were obtained or, equivalently, the radius of the hard core of the fibers as well.

It must be mentioned that unit cells of structures of nonoverlapping fibers can also be constructed by randomly introducing the fibers in the cell one by one, through random selection of the coordinates of the trace of their axes, and rejecting those that happen to overlap with fibers already placed in the cell. The random sequential addition scheme can be implemented on the computer more easily than the scheme based on the Metropolis Monte Carlo method, and it has been employed in a number of studies dealing with the two-dimensional site percolation problem. This scheme, as our computations also showed, suffers from the serious drawback of not being capable of producing nonoverlapping structures for porosities less than about 45%. Pike and Seager (1974) used this simple construction scheme to produce the unit cells used in their percolation study of partially overlapping disks on a plane, but, of course, no results were reported for hard-core porosities lower that 0.50. The technique was also used by Smith and Torquato (1988), who also reported a minimum achievable porosity of about 45%. The fiber structures obtained through random sequential addition are fundamentally different, in terms of the radial distribution functions, for instance (Widom, 1966), from those resulting through the Metropolis Monte Carlo scheme. Nevertheless, a few test calculations showed that the effective diffusivities and structural properties of these structures are, within the statistical error of our computations, practically the same. Similar conclusions were reached by Smith and Torquato from their two-point matrix probability function computations.

Because of the geometrical simplicity of the structures of nonoverlapping fibers, expressions for the dependence of their porosity, ϵ, and internal surface per unit volume, S, on the fiber radius can be obtained in a straightforward fashion. For

an n-modal, discrete distribution of fiber size, we have

$$\epsilon = 1 - \pi \sum_{i=1}^{n} l_i r_i^2; \quad S = 2\pi \sum_{i=1}^{n} l_i r_i \tag{1a,b}$$

with l_i being the length of fibers of size r_i per unit volume or the number of traces of axes of fibers of size r_i per unit of area on a cross section of the structure. For a unimodal structure, like those considered in this study, the above expressions are simplified to

$$\epsilon = 1 - \pi l r^2; \quad S = 2\pi l r \tag{2a,b}$$

Using Eqs. 2, the expressions for the dimensionless surface area of the porous medium, Sr, and the dimensionless mean intercept length, $\bar{d}/r \equiv 4\epsilon/(Sr)$, are found to be

$$Sr = 2(1-\epsilon); \quad \bar{d}/r = 2\epsilon/(1-\epsilon) \tag{3a,b}$$

For freely overlapping structures, the expressions corresponding to Eqs. 2 and 3 have the form (Tomadakis and Sotirchos, 1991)

$$\epsilon = \exp(-\pi l r^2); \quad S = 2\pi\epsilon l r \tag{4a,b}$$

$$Sr = -2\epsilon \ln\epsilon; \quad \bar{d}/r = -2/\ln\epsilon \tag{5a,b}$$

Exact closed-form expressions, like Eqs. 2–5, are not available for the structural properties of partially overlapping fibers, but Rikvold and Stell (1985a,b) used the scaled-particle theory of Reiss, Frisch, and Lebowitz (1959) to develop approximating expressions which will be presented later during discussion of our results for the structural properties of the fiber structures considered in our study.

Orientationally averaged effective diffusivities are computed using the mean square displacement, $\langle \xi^2 \rangle$, of molecules travelling in the void space of the porous medium, while the computation of effective diffusivities in a given direction is based on the mean square component of the displacement in that direction. We use the formulas

$$D_e = \frac{\langle \xi^2 \rangle}{6\tau}; \quad D_{e(x,y,\text{ or } z)} = \frac{\langle \xi^2_{x,y,\text{ or } z} \rangle}{2\tau} \tag{6a,b}$$

Equations 6a and 6b must be used for relatively large values of travel time, τ, that is after the molecules have had the opportunity to adequately sample the void space of the medium. The computation of the mean square displacement is accomplished by following the trajectories of a large number of molecules, introduced randomly and travelling independently in the unit cell. The procedure used for computing the trajectories of molecules undergoing Knudsen diffusion in a porous, capillary or fibrous, structure has been described in detail in previous publications (Burganos and Sotirchos, 1989a; Tomadakis and Sotirchos, 1991). In these articles, information is also given on how the results of the trajectory computations may be used to determine the porosity, internal surface area, accessible porosity, and accessible internal surface area of the fibrous structures.

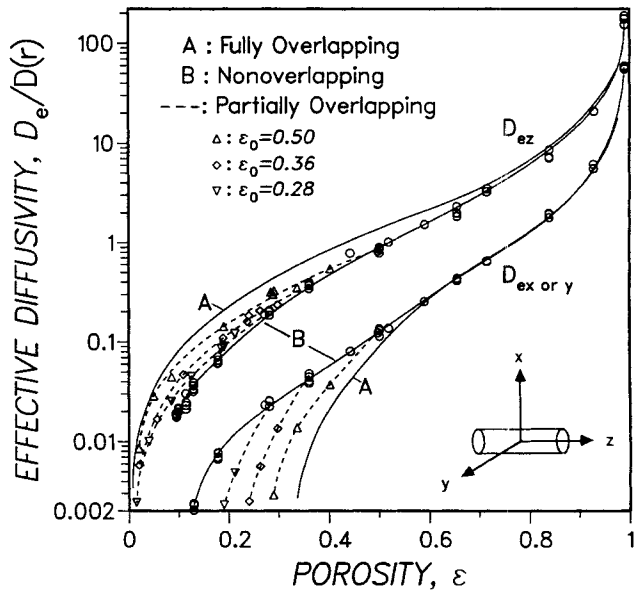

Figure 3. Effective Knudsen diffusivities in directions parallel (D_{ez}) and perpendicular (D_{ex} or D_{ey}) to the fiber axes.

$D(r) = (2/3)r\bar{v}$.

Results and Discussion

Effective Knudsen diffusivities and tortuosity factors

Our computer simulation results for the effective Knudsen diffusivities in directions parallel (D_{ez}) and perpendicular ($D_{e(x \text{ or } y)}$) to the fibers of unidirectional, unimodal fiber structures are shown in Figure 3. The fibers are allowed to be non-, partially, or freely overlapping. The last type of unidirectional fiber structures were studied in detail previously (Tomadakis and Sotirchos, 1991), and the corresponding diffusivities are shown here for comparison with those for partially overlapping fibers. As in our past studies, the effective diffusivities reported in Figure 3 and all other figures have been rendered dimensionless and independent of the fiber size using as a reference value the Knudsen diffusivity in a cylindrical pore of radius equal to the fiber radius, $D(r) = (2/3)r\bar{v}$. As the results of Figure 3 show, fibrous structures consisting of nonoverlapping fibers are characterized by lower diffusivities parallel to the fibers but higher in direction perpendicular to them than structures of freely overlapping fibers of the same fiber radius and porosity. As the porosity increases, however, the extent of fiber overlapping for the case of freely overlapping (fully penetrable) fibers decreases, and as a result, the effective diffusivities for the two cases get closer to each other and eventually coincide as the porosity approaches unity. The effective diffusion coefficient in directions perpendicular to the fibers becomes zero at porosity equal to 0.0931, the porosity of a triangular array of closely packed solid cylinders, for structures of nonoverlapping fibers, while, as Figure 3 indicates and as we have seen in our previous study, it becomes zero at a much higher porosity (~ 0.33) for freely overlapping fibers.

The different effect of fiber overlapping on the effective diffusivities in directions parallel and perpendicular to the fibers can be explained by considering the expressions for the dimensionless mean intercept length of structures of nonoverlapping and freely overlapping fiber structures presented in

the previous section (Eqs. 3b and 5b). A comparison of Eqs. 3b and 5b reveals that the dimensionless mean intercept length of nonoverlapping structures is smaller at all porosities than that of structures of freely overlapping fibers. Therefore, for the same travel distance or, equivalently, the same travel time, molecules travelling in a nonoverlapping fiber structure undergo, on the average, more collisions with the pore walls than molecules travelling in a bed of fully penetrable fibers of the same porosity, and consequently their mean square displacement and, hence, their orientationally averaged effective diffusion coefficients (see Eq. 6a) are smaller. This relationship also holds for the effective diffusivities parallel to the fibers since they are much larger than those in the other directions (see Figure 3). The effective diffusivities in directions perpendicular to the fibers behave differently because they are influenced more by the accessibility of the structure in these directions than by the frequency of molecule-wall collisions. Placing the fibers in a nonoverlapping arrangement creates more openings for mass transport perpendicularly to the fibers, and this leads to an increase in the value of the corresponding effective diffusivity.

Figure 3 also presents effective diffusivity results for partially overlapping structures. It was pointed out in the previous section that in addition to the porosity and fiber radius, partially overlapping fiber structures require for their unique identification the porosity of the nonoverlapping structure from which they were obtained, that is, their hard-core porosity. Curves for three different values of initial or hard-core porosity, ϵ_0, are shown in Figure 3. If the partially overlapping fiber structures of the figure had been obtained through a densification process, ϵ_0 would correspond to the initial porosity of the fibrous preform. Thus, notice that the curves for the partially hoverlapping structures start on the corresponding curve for nonoverlapping fibers at the hard-core porosity. The results of Figure 3 indicate that partially overlapping fiber structures exhibit behavior intermediate to that of the two extreme cases. The higher the starting porosity (ϵ_0), the closer the effective diffusivity curves are to those for freely overlapping fibers. The percolation threshold of a partially overlapping fiber structure lies between those for non- and freely overlapping fibers, that is, in the range [0.0931, 0.33], starting from 0.33 for initial porosities close to unity and approaching the porosity of a closely packed triangular array of cylinders (0.0931) as the initial porosity gets close to this value. [For porosities below the percolation threshold, no infinitely large subset of the void space that spans the porous medium perpendicularly to the fibers is present, and consequently, the corresponding effective diffusivities ($D_{e(x \text{ or } y)}$) are zero.] As we will see later, the percolation thresholds of Figure 3 are in agreement with those obtained using a fiber cluster identification method.

The data points shown in Figure 3 and all other figures represent simulation results for different random realizations of the fiber structures with each point representing the result from a single realization. Therefore, information on the statistical errors involved in our simulation may be obtained by direct inspection of the figures. The porosity of the fiber structures was varied by changing the fiber radius to unit cell side ratio, r/a, keeping the population of the fibers constant. The majority of the results reported here was obtained using 224 fibers per unit cell. Test runs using other fiber densities were carried to investigate the sensitivity of the results to this parameter. The porosity of the structures and the starting porosity for partially overlapping fibers proved to be the only parameters that systematically influenced the predicted effective diffusivities.

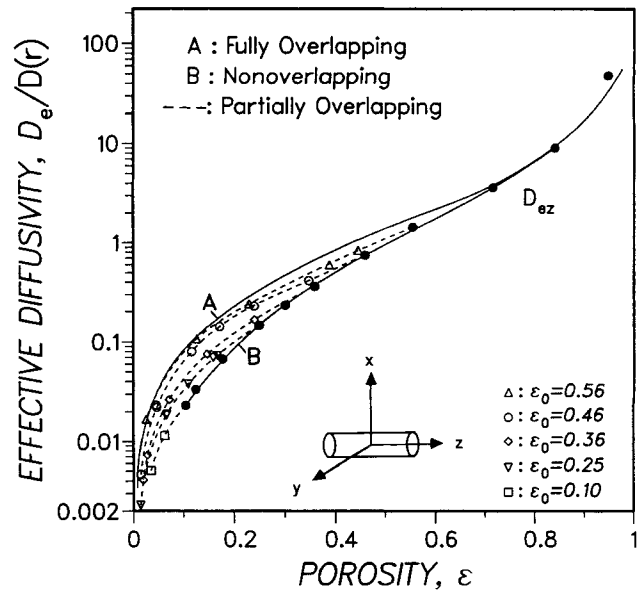

Figure 4. Effective Knudsen diffusivities parallel to the fibers (D_{ez}) obtained using Kennard's (1938) expression for nonreentrant tubes (Eq. 7).

$D(r) = (2/3)r\bar{v}$.

More results for the effective diffusion coefficients are shown in Figure 4 for diffusion parallel to the fibers. These results were obtained using an expression by Kennard (1938) for diffusion in tubes of nonreentrant shape, i.e., with walls parallel to the direction of diffusion. According to this expression,

$$\frac{D_{ez}}{D(r)} = \frac{3}{16rA} \int_A \int_0^{2\pi} s d\phi dA \tag{7}$$

For our problem, A is the cross-sectional area of the unit cell and s is the distance from the area element dA to the walls of the fiber structure on the plane of the cross section at an angle ϕ with respect to some reference line. A Monte Carlo simulation scheme was used to compute the double integral of Eq. 7 (Burganos and Sotirchos, 1988). The diffusion coefficients obtained through Eq. 7 are in excellent agreement with these of the mean square displacement method, as one can readily see by comparing Figures 3 and 4.

It was pointed out during the introduction of Eqs. 6a and 6b that the effective diffusivity in the mean square displacement method should be obtained from the slope of the $\langle \xi^2 \rangle$ or $\langle \xi^2_{x,y, \text{ or } z} \rangle$ vs. travel time curve for large values of travel time, that is, after a linear relationship between mean square displacement and travel time has been established. Burganos and Sotirchos (1989a) examined the effect of travel time on the computation of effective diffusivities in pore structures of overlapping capillaries. They found that a travel distance of the order of $150r$ was large enough to give the correct diffusivity for 94% porosity, while the required minimum travel distance was reduced to $100r$ at $\epsilon = 0.83$ and $80r$ at $\epsilon = 0.50$. (The travel

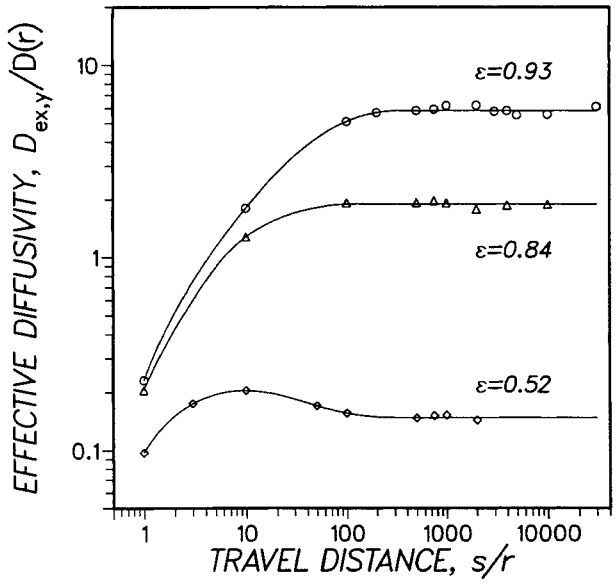

Figure 5. Dependence of computed effective diffusivities ($D_{e(x \text{ or } y)}$) from the mean square displacement equation (Eq. 6b) in nonoverlapping fibers on the dimensionless travel distance of the molecules.

$D(r) = (2/3)r\bar{v}$.

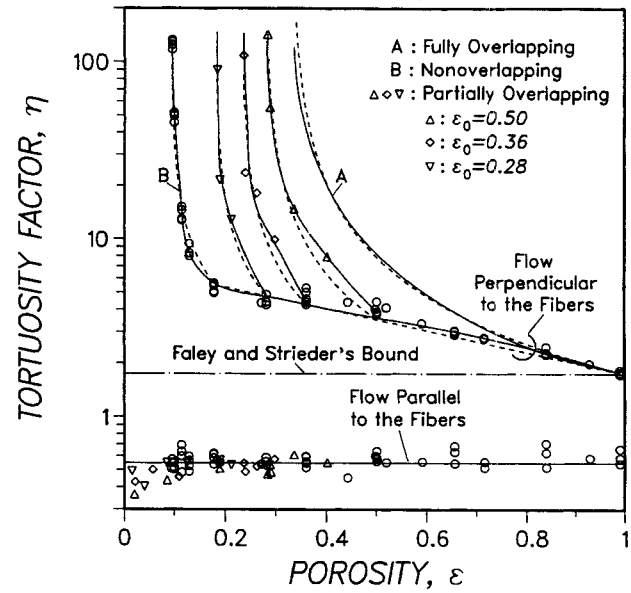

Figure 6. Variation of the tortuosity factor with respect to the Knudsen diffusivity based on $\bar{r} = 2\epsilon/S$ with the porosity for effective diffusivity results of Figure 3.

The dashed curves are predicted by the correlations given by Eqs. 9-11.

distance, s, is defined as the product of the thermal speed of the molecules and the travel time, i.e., $s = \bar{v}\tau$.) An investigation of the effects of travel distance on the computed effective diffusivities was also carried out in this study for the beds of nonoverlapping fibers, and the results obtained are shown in Figure 5. The effective diffusivities shown in the figure were obtained by simply dividing the mean square displacement by 2τ, that is, without taking the slope of the $\langle \xi^2_{x \text{ or } y} \rangle$ vs. τ curve. The results of Figure 5 indicate that the minimum travel distance increases with increasing porosity and are thus in relative agreement with those of Burganos and Sotirchos (1989a). The minimum travel distance at a given porosity tends, in general, to be higher for fibers, indicating that molecules travelling in fibrous structures need more time to adequately sample the void space, especially at high porosities.

It should be pointed out that the above values of travel distance suffice for the computation of the effective diffusivity in the absence of inaccessible regions of void space for diffusion perpendicularly to the fibers. When such regions are present, in partially or freely overlapping fiber structures, travel distances of the order of $10^4 r$ to $10^5 r$ may have to be used in order to be able to distinguish between permanently and temporarily trapped molecules in the pore space.

The effective diffusivity data of Figures 3 and 4 can be expressed in terms of a tortuosity factor by using the Knudsen diffusivity based on the average radius $\bar{r} = \bar{d}/2$ as reference, that is by writing

$$D_{ei} = \frac{\epsilon}{\eta_i} D(\bar{r}); \quad \frac{D_{ei}}{D(r)} = \frac{\epsilon}{2\eta_i} \frac{\bar{d}}{r}, \quad i = x,y,z \qquad (8a,b)$$

with $\bar{d}/r$ given by Eqs. 3b and 5b for nonoverlapping and freely overlapping fibers, respectively. The dimensionless mean intercept length that was obtained from the results of our molecular trajectory computations was used in Eq. 8b to determine the tortuosity factors. The computed tortuosity factors are plotted in Figure 6 as functions of the total porosity. The tortuosity factors for diffusion perpendicularly to the fibers increase with decreasing porosity and become infinitely large as the percolation threshold is approached. In the vicinity of 100% porosity, the tortuosity factors for all cases approach the lower bound ($\eta = 1.747$) that was derived by Faley and Strieder (1987) for diffusion perpendicularly to freely overlapping fibers. The tortuosity factor for diffusion parallel to the direction of the fibers was found to exhibit weak dependence on the porosity and the extent of fiber overlapping. For the 75 realizations of non- and partially overlapping fibers shown in the figure, it had an average value of 0.547, which is almost identical to that estimated in our previous study (Tomadakis and Sotirchos, 1991) for freely overlapping fibers ($\eta = 0.549$).

In order to facilitate use of our diffusivity results by people working on problems involving transport in fibrous beds, we developed in our work on the diffusivities of freely overlapping fibers (Tomadakis and Sotirchos, 1991), a one parameter-correlation that could be used to relate the various tortuosity factors to the porosity of the medium. A similar expression of the form

$$\eta = \eta(\epsilon_0) \left(\frac{\epsilon_0 - \epsilon_p}{\epsilon - \epsilon_p} \right)^{\alpha} \qquad (9)$$

was used here to correlate the tortuosity factor (for diffusion perpendicularly to the fibers) vs. porosity results of Figure 6. ϵ_0 is the hard-core porosity of the fibers, i.e., the porosity at the point where the tortuosity factor curves for partially over-

lapping structures leave the curve for nonoverlapping fibers, $\eta(\epsilon_0)$ is the corresponding tortuosity factor, and ϵ_p is the percolation threshold. The dependence of ϵ_p on ϵ_0 is given in Figure 11, which is discussed in the following section. α was determined for each case through nonlinear regression on the data of Figure 6. We found that α and ϵ_p could be correlated by the linear expression

$$\alpha = 2.28\epsilon_p + 0.35 \tag{10}$$

with 99.93% correlation coefficient. The results for the tortuosity factor of nonoverlapping fibers were correlated for $\epsilon \geq 0.18$ by the exponential expression

$$\eta = 1.747\exp[1.4(1-\epsilon)] \tag{11}$$

The data for lower porosities were approximated by Eq. 9 with $\epsilon_0 = 0.18$, $\epsilon_p = 0.0931$ and $\alpha = 0.72$. The results predicted by Eqs. 9-11 for all cases considered in Figure 6 are shown by dashed curves. Notice that for $\epsilon_0 = 1$ and $\eta(\epsilon_0) = 1.747$ (Faley and Strieder's variational bound), Eqs. 9 and 10 yield the correlation presented in our previous article (Tomadakis and Sotirchos, 1991) for freely overlapping fibers.

Results for the structural properties

On the basis of the scaled-particle theory of hard sphere fluids of Reiss et al. (1959) and its extension to lower dimensions, Rikvold and Stell (1985a,b) derived approximate expressions for the porosity and surface area of porous structures consisting of partially overlapping (penetrable) spheres or unidirectional cylinders. For the case of unidirectional cylinders, their expressions, written in the notation employed in this study, have the form

$$\epsilon = \epsilon_0\exp[(\delta^2-1)(1-1/\epsilon_0) - (\delta-1)^2(1-1/\epsilon_0)^2] \tag{12}$$

$$Sr = 2\epsilon\delta(1-1/\epsilon_0)\left(\frac{1-\delta}{\epsilon_0}-1\right) \tag{13}$$

δ is the fiber growth variable, i.e., the ratio of the fiber radius to the hard-core radius ($\delta = r/r_0$). Equations 12 and 13 may be used to obtain the following approximation for the mean intercept length of partially overlapping fiber structures:

$$\frac{\bar{d}}{r} \equiv \frac{4\epsilon}{Sr} = 2\left[\delta\left(1-\frac{1}{\epsilon_0}\right)\left(\frac{1-\delta}{\epsilon_0}-1\right)\right]^{-1} \tag{14}$$

For the case of nonoverlapping fiber structures ($\delta = 1$ and $\epsilon = \epsilon_0$), Eqs. 13 and 14 are simplified to Eqs. 3a and 3b, while for freely overlapping fibers ($\delta \to \infty$ and $\epsilon_0 \to 1$), Eqs. 12-14 become indeterminate.

The predictions of Eq. 12 are compared with results obtained in this study in Figure 7. The porosity of a realization of a partially overlapping fiber structure was computed by introducing 10^5 molecules randomly into the unit cell and determining the fraction of the molecules that were found to lie in the void space. The porosity vs. fiber growth data of Figure 7 for different hard-core porosities (open circle points)—the hard-core porosity is the total porosity for $\delta = 1$—were obtained

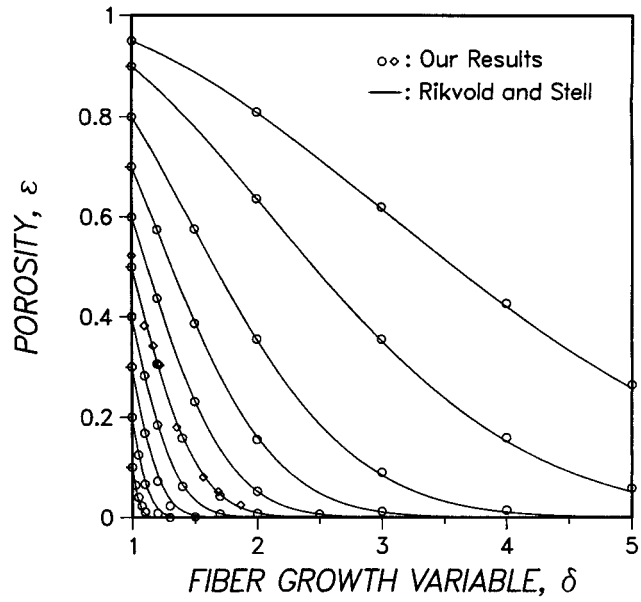

Figure 7. Comparison of computed porosities with those predicted by the scaled-particle approximation (Eq. 12).

The hard-core porosity for each curve is the porosity for $\delta = 1$.

as the average of the porosities of 30 different realizations of the same hard-core porosity and fiber growth. The Monte Carlo simulation scheme discussed in the previous section was used to construct the unit cells (224 fibers per cell) employed in the porosity computations. The first realization of each set was constructed after 500 cycles of fiber moves, while 50 cycles were used to obtain each of the subsequent realizations.

The porosity of structures consisting of nonoverlapping fibers is exactly known, and consequently, the simulation results for these structures were used to assess the accuracy and repeatability of the method used for the computation of the porosity. It was found that the estimated hard-core porosity differed by less than 0.2% from the exact value for porosities in the range [0.1, 0.95], with the largest deviations occurring in the low porosity region. The absolute standard deviation of the hard-core porosity for the 30 realizations employed in the computations varied insignificantly with the porosity, having an average value of 0.0012 for porosities in the above range. The absolute standard deviations for the porosities of partially overlapping fiber structures were comparable to those for the hard-core porosity (i.e., the porosity of nonoverlapping fibers) even though in this case different realizations of the same fiber density could have different porosities. Only for large values of the fiber growth variable ($\delta > 2$), the computed standard deviations were markedly larger than those for nonoverlapping fibers. The relative standard deviation increased significantly with decreasing porosity, that is, with increasing fiber growth and decreasing hard-core porosity. For example, at $\epsilon_0 = 0.4$, the relative standard deviation increased from 0.37% for $\delta = 1$ ($\epsilon = \epsilon_0$) to 19.7% for $\delta = 1.7$ ($\epsilon = 0.0066$). The weak dependence of the computed porosity on the realization is also evident from the data points represented using diamonds in Figure 7, which give the porosities for the realizations that were used to obtain the effective diffusivity results of Figure 3 for $\epsilon_0 = 0.50$. Notice that each of these points was computed from a single

realization and that only $500/\epsilon$ test molecules were used for the computation.

The results of Figure 7 show that the scaled-particle approximation (Eq. 12) provides a very good approximation to the porosity of partially overlapping structures for most values of hard-core porosity and fiber growth variable. For large values of ϵ_0 and large values of δ, Eq. 12 predicts smaller porosities than those found in our simulations, but the observed differences are in most cases within the standard deviation of our estimates. For $\delta=4$ and $\epsilon_0=0.9$, for instance, the difference between our porosity estimate and the prediction of Eq. 12 is 4.5%, while the standard deviation of our result is about 9%. Away from the lower bound of the range of hard-core porosities (that is, away from $\epsilon_0=0.0931$), Eq. 12 overpredicts the porosity of partially overlapping fiber structures for δ values smaller than 2, the differences being, in general, much larger than the standard deviation of our estimates but still relatively insignificant on an absolute scale. The largest relative deviations between our results and the predictions of Eq. 12 are encountered in the vicinity of the lower bound of hard-core porosity, where Eq. 12 tends to underpredict the porosity. This behavior is not surprising since the existence of a finite lower bound on ϵ_0 is not predicted by Eq. 12.

The variation of the dimensionless surface area of structures of unisized fibers with the porosity is shown in Figure 8. The surface areas plotted in the figure are those computed for the realizations used to obtain the results of Figure 3. They were estimated using the dimensionless mean intercept length $\bar{d}/r$ of the fibrous structure and the relationship $Sr=4\epsilon/(\bar{d}/r)$. The variation of the mean intercept length of the structures of Figure 3 with the porosity is shown in Figure 9. The mean intercept length was computed as the arithmetic mean of the paths between molecule-wall collisions for the molecules used in our Knudsen diffusivity computations, with all molecules allowed to travel in the void space for the same time. The Sr vs. ϵ curve given by Eq. 5a for freely overlapping fibers is shown in Figure 8 for comparison. The predictions of Eq. 5a were compared with our simulation results in our previous study (Tomadakis and Sotirchos, 1991), and excellent agreement was found to exist. For nonoverlapping fibers, Eq. 3a predicts a linear relationship between Sr and ϵ, and as the results of Figure 8 show, this relationship is also obeyed by the simulation results obtained in our study. However, significant differences are found to exist between the computed surface areas for partially overlapping fiber structures and those predicted by the relationship developed by Rikvold and Stell (1985a,b) (Eq. 13). The relative differences between Eq. 13 and the simulation results appear to increase with decreasing hard-core porosity and increasing densification. Such a behavior is in qualitative agreement with that seen for the porosity results of Figure 7. Notice that the internal surface area of nonoverlapping fiber structures has a tendency to increase at the onset of fiber growth, but the loss of surface area that takes place as the fibers start to grow into each other eventually offsets the gain caused by fiber growth.

The overall structural properties of partially overlapping cylinders or disks on a plane were also studied by other investigators. Lee and Torquato (1988a) used various simulation procedures, including one similar to that employed here, to compute the porosity of structures consisting of partially penetrable (overlapping) spheres or unidirectional cylinders. Their

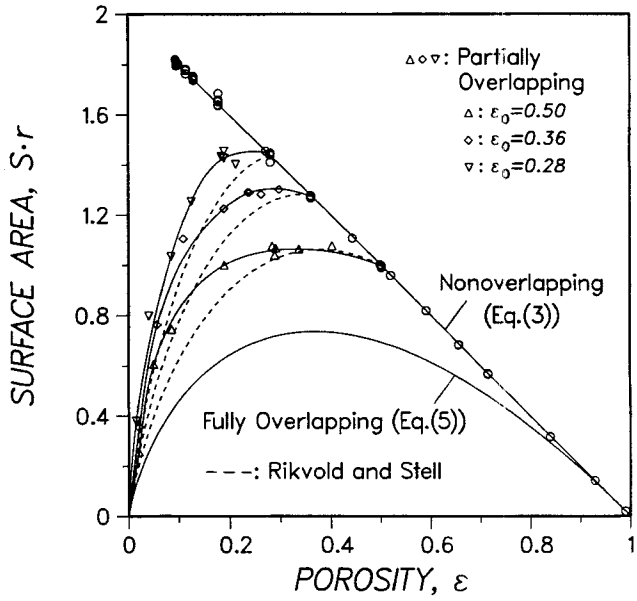

Figure 8. Internal surface vs. porosity results for the structures of Figure 3 and comparison with predictions of the scaled-particle approximation (Eq. 13).

results for unidirectional cylinders are in very good agreement with those obtained in our study, and the same also holds for their conclusions on the predictions of Eq. 12. However, Lee and Torquato concentrated their efforts in the region of $\delta<3.3$ and $\epsilon_0>0.3$, and as a result, they did not encounter underestimation of the porosity by Eq. 12. Smith and Torquato (1988) used computer simulation estimates of the slope of the two-point matrix probability function to compute the internal surface area of structures made up by non-, partially, or freely overlapping cylinders. Their results were reported in the form of Sr vs. ϵ curves for five different values of δ (λ^{-1} in their notation), and consequently, they are not directly comparable

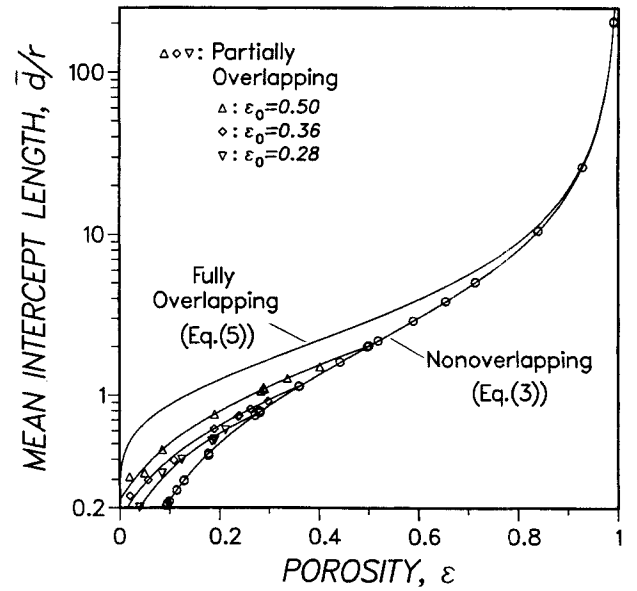

Figure 9. Mean intercept length vs. porosity results for the structures of Figure 3.

with ours. We used the results of Figure 7 to determine the hard-core porosities for the (ϵ,δ) pairs used by Smith and Torquato, and the values of ϵ, δ, and ϵ_0 were then used in Eq. 13 to find the *Sr* values predicted by the approximation developed by Rikvold and Stell (1985a,b). It was found that the results of Smith and Torquato were higher than the predictions of Eq. 13 in the low porosity region (by about 7% for the two data points they report between 10 and 20% porosity), but much better agreement was observed for the results at higher porosities. This behavior is in accordance with that observed for our results in Figure 8.

It was pointed out during the discussion of the effective diffusivity results that unidirectional fiber structures become inaccessible to diffusion perpendicularly to the fibers below some porosity level, usually referred to as their percolation threshold. A partially overlapping fiber structure that is impermeable to diffusing molecules perpendicularly to the fibers is shown in Figure 2. As mentioned before, this structure has a hard-core porosity of 45%, that is, the porosity of the nonoverlapping fiber structure of Figure 1A from which it originates, and fiber growth of 25% which is over the 18% level at which structures of partially overlapping fibers with 45% hard-core porosity become inaccessible, on the average. In most practical applications mass transport usually takes place perpendicularly to the fibers, and consequently, the percolation threshold of unidirectional fiber structures is one of their most important structural characteristics. For instance, if the fibrous bed is going to serve as a preform in a densification process, knowledge of its percolation threshold enables us to obtain a good estimate of the minimum achievable porosity.

The percolation threshold of a unidirectional fiber structure, perpendicularly to the fibers, can be approximated by the maximum porosity value at which the corresponding diffusion coefficient ($D_{e(x \text{ or } y)}$ in our notation) is zero. However, a very large number of test molecules and very large travel times must be employed to obtain an accurate estimate of the percolation threshold using this method. Such a method may be the only recourse for other types of fiber structures (for example, randomly oriented), but for unidirectional fiber structures one may use a much faster scheme, whose development makes use of the fact that in such structures the percolation thresholds of the void and solid regions are located at the same porosity value. The accessibility of the solid part of the porous medium can be studied by using a procedure to identify clusters of fibers and determine whether infinitely large clusters spanning the space perpendicularly to the fibers are present (Pike and Seager, 1974). For the finite unit cell used in our study, existence of infinitely large clusters is understood as the situation in which clusters that include boundary fibers from a pair of opposite faces of the cell, are present. A cluster identification scheme was also used by Burganos and Sotirchos (1989b) to study the percolation characteristics of unidirectional capillaries overlapping with an assemblage of spherical cavities.

We used the above described cluster identification procedure to locate the percolation thresholds of freely or partially overlapping fiber structures. The unit cells were constructed as explained before, and the realizations were sampled as in the case of our porosity calculations (Figure 7). Once a nonoverlapping fiber structure was constructed, the fibers were grown in discrete steps, and each new structure was checked for the existence of infinite clusters of fibers. After a structure with

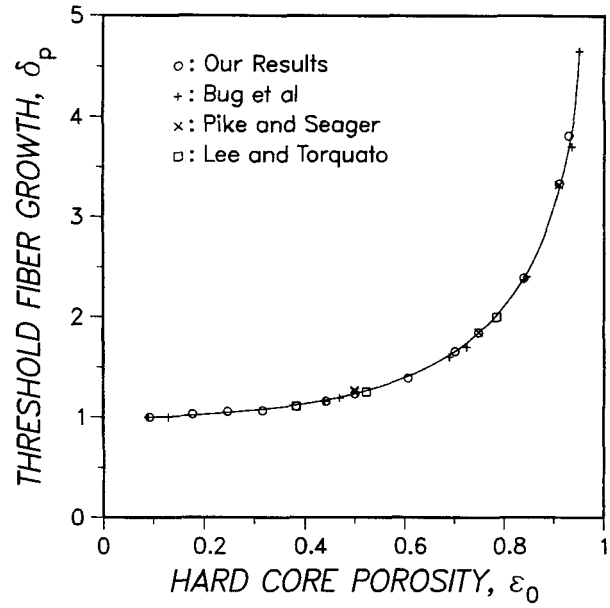

Figure 10. Variation of the value of the fiber growth variable at the percolation threshold, δ_p, with the hard-core porosity for partially-overlapping fiber structures.

infinite fiber clusters was encountered, smaller growth steps were used between this structure and the previous one, and the resulting structures were again checked for infinite clusters. This process was repeated until the value of the growth variable at which formation of infinite clusters first took place, δ_p, was located within 0.001%. The corresponding porosity threshold, ϵ_p, was then determined as the probability that a molecule introduced randomly in the structure falls in the void space. As in all other cases, 224 fibers were used in the computations, and for a given hard-core porosity, the percolation threshold was computed as the average of 25 realizations. The effect of fiber density (per cell) on the computations was investigated in detail for the case of freely overlapping fibers in our previous study (Tomadakis and Sotirchos, 1991), where it was concluded that a population density of the order of 200 fibers per cell suffices for a satisfactory estimation of the threshold porosity. For 200 fibers per cell, the percolation threshold of randomly overlapping fibers for 50 realizations had an average value of 0.329 and a standard deviation of 0.045.

Our results for the growth variable at the percolation threshold, δ_p, as a function of the initial (hard-core) porosity, ϵ_0, are given in Figure 10, along with (ϵ_0, δ_p) data compiled from other studies of the literature. Each of our δ_p values shown in the figure is the average of the results for 25 different realizations. Test runs for a few cases showed that the average values were practically independent of the sample size, in agreement with the conclusions for freely overlapping fibers. The standard deviation of δ_p values of different realizations—all consisting of 224 fibers and having the same hard-core porosity—was found to be insignificant (less than 1%) for $\epsilon_0 < 0.3$. At a hard-core porosity of 50% this deviation is still small, of the order of 3%, but grows to 6% at $\epsilon_0 = 0.7$ and 9% at $\epsilon_0 = 0.9$. The variation of the threshold porosity, ϵ_p, with the initial or hard-core porosity, ϵ_0, is shown in Figure 11, where the only analogous results found in the literature (Lee and Torquato, 1988b)

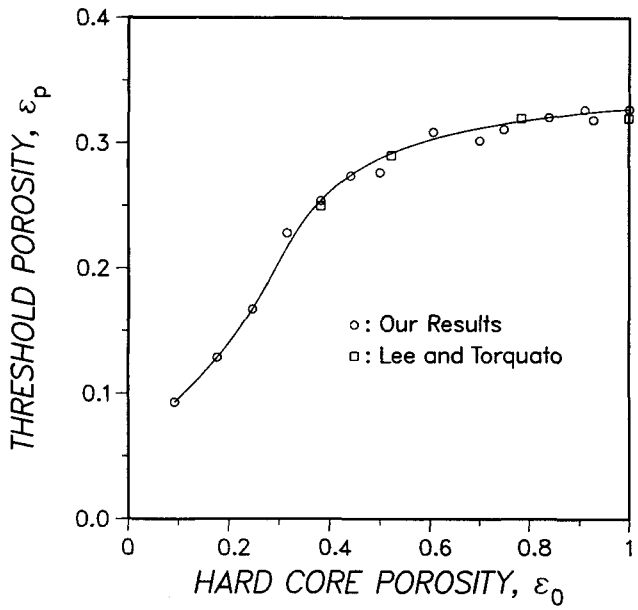

Figure 11. Variation of the porosity at the percolation threshold, ϵ_p, with the hard-core porosity for partially-overlapping fiber structures.

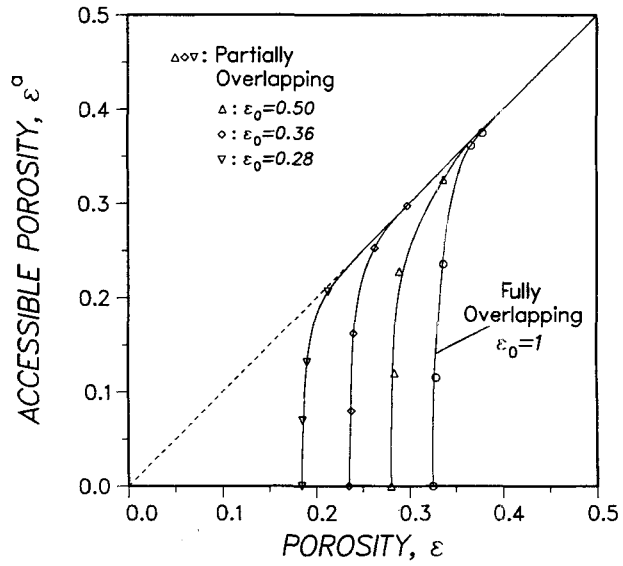

Figure 12. Variation of the accessible porosity with the total porosity.

are also shown. Actually, it is the three data points of Figure 11 that we have plotted in Figure 10, after using the results of a previous study of the authors (Lee and Torquato, 1988a) to convert them to the (ϵ_0, δ_p) form.

Pike and Seager (1974) used a cluster identification method to obtain the results they reported. They worked with samples of 400–1,000 disks on a plane and averaged over 8–22 realizations. They observed weak dependence of the average δ_p on the sample size but decreasing standard deviation with increasing sample size. Bug et al. (1985) obtained their results by applying a Monte Carlo simulation method to examine the effects of particle interactions on the percolation thresholds of structures consisting of spherical or unidirectional cylindrical, partially permeable particles. Finally, the results of Lee and Torquato (1988b) were obtained using simulation results for pair-connectedness and mean cluster size in structures of partially penetrable spheres or unidirectional cylinders. Lee and Torquato presented results for different sample sizes, which, in agreement with our and Pike and Seager's results, suggest there is no need for more than 200 fibers per cell to obtain a satisfactory estimate of the percolation threshold.

It should be pointed out that periodic boundary conditions were used in the construction of the finite samples used in our percolation studies and the other studies of the literature. We investigated the effect of boundary conditions by carrying out cluster identification studies on unit cells that did not include boundary fibers from neighboring cells. The average threshold value of the growth variable was about 0.4% higher in the absence of boundary conditions, while its standard deviation practically remained the same as that for cells with periodic boundary conditions.

In addition to the above mentioned studies, some studies have focused on the derivation of approximations for the percolation threshold of interacting disks on a plane. Such approximations are usually successful in predicting the qualitative behavior of δ_p as a function of ϵ_0, but they exhibit significant quantitative differences from the results of Monte Carlo simulation studies, especially for low hard-core porosities (Stauffer, 1985). For instance, Odagaki and Lax (1987) used the coherent medium approximation to obtain a theoretical result, which could be transformed to a relation between the δ_p and ϵ_0 variables defined in our study. However, their approach does not predict the lower limit on the porosity of structures of nonoverlapping fibers ($\epsilon_{ocp}=0.0931$), and it overestimates δ_p by a significant amount (e.g., by about 50% for $\epsilon_0=0.35$ and 25% for $\epsilon_0=0.80$).

The densification level at which a fibrous bed of unidirectional fibers becomes inaccessible to diffusion perpendicularly to the fibers is a very important structure characteristic, but for practical applications, one should also know the variation of the inaccessible porosity with the extent of densification. Accessible porosity vs. total porosity results for the three values of hard-core porosity considered in Figure 3 and for a structure of freely overlapping fibers (Tomadakis and Sotirchos, 1991) are shown in Figure 12. Accessible porosities were determined by using the molecular trajectory computations to determine the fraction of molecules travelling in isolated regions of the pore space. The details of the procedure used for this computation, as well as its limitations, are described in some detail by Tomadakis and Sotirchos (1991). As in our previous study, very large travel times (more than 2×10^5 molecule-wall collisions) were used near the percolation thresholds. The behavior of the accessible vs. total porosity curves of partially overlapping fibers is similar to that of a freely overlapping fiber structure. In all cases, formation of inaccessible pore space starts and ends within a very narrow range of porosity. It was mentioned during the presentation of the results for the percolation threshold that for a sample size of about 200 fibers, the average percolation threshold presents a relative standard deviation of about 13%. Therefore, to obtain accessible porosity results representative of the average behavior of the system, it was decided to work with fiber structures that become inaccessible at the average porosity level found, for each ϵ_0, from our cluster identification studies.

Summary and Conclusions

A numerical investigation of the Knudsen diffusion and percolation behavior of porous structures consisting of parallel, nonoverlapping or partially overlapping fibers was carried out. The construction of the finite unit cells employed in our simulation studies was accomplished using a scheme based on the Metropolis Monte Carlo simulation method. Partially overlapping fiber structures were constructed from structures of nonoverlapping fibers through fiber growth and effective diffusivities were computed using the mean square displacement of molecules travelling in the porous medium for large times. The mean square displacement was determined using a Monte Carlo simulation process based on following the trajectories of a large number of molecules, each travelling independently, introduced randomly in the unit cell of the fibrous bed. Using a method proposed by Burganos and Sotirchos (1989c), the computed molecular trajectories were also used to obtain estimates of the accessible porosity and accessible internal surface area of the structures. Appropriate boundary conditions were used to construct periodic unit cells and thus be able to obtain diffusivity results representative of the infinite medium. Ability to work in an infinite medium is essential for obtaining accurate estimates of the mean square displacement and, hence, of the effective diffusion coefficient.

Our results showed that fibrous structures consisting of nonoverlapping fibers exhibit lower diffusivities parallel to the fibers but higher in directions perpendicular to them than structures made of freely overlapping fibers of the same radius and porosity. Structures of partially overlapping fibers show behavior intermediate to those of the two extreme cases. The observed differences among the diffusivities of non-, freely, and partially overlapping fiber structures decrease as the porosity increases and the extent of fiber overlapping is reduced, vanishing as the porosity approaches unity. The tortuosity factor with respect to the Knudsen diffusion coefficient based on the average pore radius $\bar{r}=2\epsilon/S$ is almost constant for diffusion parallel to the fibers regardless of the extent of fiber overlapping, having an average value of about 0.55, that is, the same as in the case of freely overlapping fibers (Tomadakis and Sotirchos, 1991). For diffusion perpendicularly to the fibers, on the other hand, the tortuosity factor increases with decreasing porosity from a minimum value corresponding to the upper bound on the effective diffusivity that is derived through variational principles (Faley and Strieder, 1987), and diverges to infinity as the percolation threshold of the fibrous bed (that is, the porosity level below which the pore space of the sample is inaccessible to diffusion perpendicularly to the fibers) is approached.

Because of the importance of the percolation threshold of a fibrous bed in practical applications, a simulation method based on the identification of clusters of fibers in the unit cell of the structure was used for its more accurate estimation. Our results showed that the percolation threshold of partially overlapping fibrous structures decreases with decreasing hard-core porosity, i.e., the porosity of the structure made of the nonoverlapping fiber cores, varying in the range [0.0931, 0.33]. The lower bound is the porosity of a closely packed triangular array of nonoverlapping fibers—where threshold porosity is equal to the hard-core porosity—while the upper bound corresponds to the percolation threshold of a structure of freely overlapping fibers—where the hard-core porosity is equal to unity. The results of our cluster identification studies were in agreement with those suggested by our effective diffusivity measurements and with the results of other studies of the literature.

As the porosity decreases (because of a densification process, for example), formation of inaccessible porosity perpendicularly to the fibers in partially or freely overlapping fiber structures starts and becomes completed within a very narrow range of porosity. Consequently, the accessible porosity and internal surface area may be approximated, for most practical purposes, by the total values of porosity and surface area in the porosity range above the percolation threshold. The computed values of total porosity and internal surface area of nonoverlapping or freely overlapping fiber structures were in excellent agreement with the theoretically predicted values, indicating that the finite samples used in our simulations were statistically representative of the infinite media. The variation of the porosity and surface area of partially overlapping structures with the hard-core porosity and fiber growth was found to be in good qualitative agreement with that predicted by approximations derived by Rikvold and Stell (1985a,b). The quantitative agreement was also good, and in some cases excellent, for large total and hard-core porosities, but significant quantitative differences existed for the surface area in the low porosity region.

Acknowledgment

The authors would like to thank the Pittsburgh Supercomputing Center for providing supercomputer time for the computations reported here.

Notation

a = side of the cubic unit cell, m
$\bar{d}$ = mean intercept length ($\bar{d}=4\epsilon/S$), m
$D(r)$ = Knudsen diffusivity in a cylindrical capillary of radius r, m^2/s
D_e = effective diffusivity, m^2/s
l_i = length of axes per unit volume of fiber of radius r_i, m/m^3
r = fiber radius, m
r_o = hard-core radius, m
$\bar{r}$ = average pore radius ($\bar{r}=2\epsilon/S$), m
S = internal surface area, m^2/m^3
$\bar{v}$ = mean thermal speed of the molecules, m/s

Greek letters

δ = fiber growth variable ($\delta=r/r_o$)
ϵ = porosity
ϵ_0 = hard-core porosity
η = tortuosity factor
$\langle\xi^2\rangle$ = mean square displacement, m^2
τ = travel time, s

Subscripts

0 = initial (hard-core) structural properties
ocp = ordered close packing of fibers
p = structural properties at the onset of percolation
rcp = random close packing of fibers
x, y, z = x-, y- or z-direction

Literature Cited

Berryman, J. G., "Random Close Packing of Hard Spheres and Disks," *Phys. Rev. A*, **27**, 1053 (1983).

Bug, A. L. R., S. A. Safran, G. S. Grest, and I. Webman, "Do Interactions Raise or Lower a Percolation Threshold?" *Phys. Rev. Let.*, **55**, 1896 (1985).

Burganos, V. N., and S. V. Sotirchos, "Simulation of Knudsen Diffusion in Random Networks of Parallel Pores," *Chem. Eng. Sci.*, **43**, 1685 (1988).

Burganos, V. N., and S. V. Sotirchos, "Knudsen Diffusion in Parallel, Multidimensional or Randomly Oriented Capillary Structures," *Chem. Eng. Sci.*, ***44***, 2451 (1989a).

Burganos, V. N., and S. V. Sotirchos, "Effective Diffusivities in Cylindrical Capillary-Spherical Cavity Pore Structures," *Chem. Eng. Commun.*, **44**, 2629 (1989b).

Burganos, V. N., and S. V. Sotirchos, "Fragmentation of Random Pore Structures," *Chem. Eng. Commun.*, **85**, 95 (1989c).

Caputo, A. J., W. J. Lackey, and D. P. Stinton, "Development of a New Faster Process for the Fabrication of Ceramic Fiber-Reinforced Ceramic Composites by Chemical Vapor Infiltration," *Proc. 9th Ann. Conf. Comp. and Adv. Ceram. Mater.*, F. D. Gac, ed., p. 694, The Am. Cer. Soc., Columbus, OH (1985).

Faley, T. L., and W. Strieder, "Knudsen Flow through a Random Bed of Unidirectional Fibers," *J. Appl. Phys.*, **62**, 4394 (1987).

Hopkins, G. R., and J. Chin, "SiC Matrix/SiC Fiber Composite: A High-Heat Flux, Low Activation, Structural Material," *J. Nucl. Mat.*, **143**, 148 (1986).

Kennard, E. H., *Kinetic Theory of Gases*, McGraw-Hill, New York (1938).

Lee, S. B., and S. Torquato, "Porosity for the Penetrable-Concentric-Shell Model of Two-Phase Disordered Media: Computer Simulation Results," *J. Chem. Phys.*, **89**, 3258 (1988a).

Lee, S. B., and S. Torquato, "Pair Connectedness and Mean Cluster Size for Continuum-Percolation Models: Computer Simulation Results," *J. Chem. Phys.*, **89**, 6427 (1988b).

Metropolis, N., A. W. Rosenbluth, M. N. Rosenbluth, A. H. Teller, and E. Teller, "Equations of State Calculations by Fast Computing Machines," *J. Chem. Phys.*, **21**, 1087 (1953).

Meyers, M. A., and K. K. Chawla, *Mechanical Metallurgy Principles and Applications*, Prentice-Hall, Englewood Cliffs, NJ (1984).

Naslain, R., F. Langlais, and R. Fedou, "The CVI-Processing of Ceramic Matrix Composites," *Journal de Physique*, **50**, C5-191 (1989).

Odagaki, T., and M. Lax, "Percolation in Spatially Disordered Systems," *Phys. Rev. B*, **36**, 3851 (1987).

Pike, G. E., and C. H. Seager, "Percolation and Conductivity: A Computer Study. I," *Phys. Rev. B*, **10**, 1421 (1974).

Reiss, H., H. L. Frisch, and J. L. Lebowitz, "Statistical Mechanics of Rigid Spheres," *J. Chem. Phys.*, **31**, 369 (1959).

Rikvold, P. A., and G. Stell, "Porosity and Specific Surface for Interpenetrable-Sphere Models of Two-Phase Random Media," *J. Chem. Phys.*, **82**, 1014 (1985a).

Rikvold, P. A., and G. Stell, "D-Dimensional Interpenetrable-Sphere Models of Random Two-Phase Media: Microstructure and an Application to Chromatography," *J. Col. Int. Sci.*, **108**, 158 (1985b).

Smith, P., and S. Torquato, "Computer Simulation Results for the Two-Point Probability Function of Composite Media," *J. Comp. Phys.*, **76**, 176 (1988).

Stauffer, D., *Introduction to Percolation Theory*, Taylor and Francis, Philadelphia (1985).

Tomadakis, M. M., and S. V. Sotirchos, "Effective Knudsen Diffusivities in Structures of Randomly Overlapping Fibers," *AIChE J.*, **37**, 74 (1991).

Widom, B., "Random Sequential Addition of Hard Spheres to a Volume," *J. Chem. Phys.*, **44**, 3888 (1966).

Manuscript received Dec. 27, 1990, and revision received June 12, 1991.